eng

MDPI

Article

Waveform Analysis of Non-Sinusoidal Electrical Signals Using Cubic Spline Interpolation

Yaroslav Shklyarskiy [1], Olga Bolshunova [2] and Yuliya Kuznetsova [1,*]

[1] Department of General Electric Engineering, Empress Catherine II Saint Petersburg Mining University, St. Petersburg 199106, Russia
[2] Scientific and Pedagogical Center "Postgraduate Studies", Empress Catherine II Saint Petersburg Mining University, St. Petersburg 199106, Russia
* Correspondence: kuznetsova-yuliya01@yandex.ru

Abstract

The steady increase in nonlinear loads in modern electric power systems leads to distortion of electrical signal waveforms and, consequently, to deterioration of power quality. The presence of higher harmonics in the network adversely affects electrical equipment, especially capacitor banks. The classical harmonic analysis method based on the discrete Fourier transform has a number of drawbacks; therefore, the authors propose a new approach to analyzing voltage and current waveforms using cubic spline interpolation, which has not previously been applied as an independent method for analyzing electrical signals. The paper examines in detail the application of harmonic analysis and spline interpolation methods for standard equivalent circuits of loads: with a resistive-inductive load and with a connected capacitor bank. Computer simulation using Multisim software revealed that spline interpolation not only achieves accuracy comparable to that of harmonic analysis but also outperforms it when analyzing supply voltage waveforms at the connection point and current waveforms flowing through the capacitor bank, including when interharmonics are present in the network. Thus, the approach presented in the paper, based on the use of spline interpolation, can be recommended for application in the design, calculation, and reliability assessment of power supply systems, as well as in power quality monitoring and metering.

Keywords: power quality; harmonic analysis; discrete Fourier transform; spline interpolation; capacitor banks

Check for updates

Academic Editors: Gian Giuseppe Soma and Sergio Spanò

Received: 21 August 2026
Revised: 12 October 2026
Accepted: 13 October 2026
Published: 16 October 2026

Copyright: © 2026 by the authors. Licensee MDPI, Basel, Switzerland. This article is an open access article distributed under the terms and conditions of the Creative Commons Attribution (CC BY) license.

1. Introduction

A characteristic feature of modern electric power systems is the increasing share of nonlinear loads, caused by the widespread adoption of power electronics, variable-frequency drives, renewable energy sources, and other electrical equipment [1–3]. As a result, the instantaneous voltage and current waveforms become distorted; thus, the voltage and current waveforms are non-sinusoidal [4–6]. Such distortions lead to adverse consequences, including damage to cable insulation, overheating of electric motors, and incorrect tripping of circuit breakers [7]. Distortions of voltage and current waveforms are particularly dangerous for capacitors—they cause damage to the dielectric and may even lead to a capacitor explosion [8]. In this regard, power quality monitoring is becoming one of the key tasks for power supply utilities, necessary for increasing the reliability and energy efficiency of power supply [9–11]; power quality monitoring is especially promising for industrial enterprises [12–14], and in particular for the mining sector [15].

Power quality and, in particular, the degree of voltage non-sinusoidality are governed by various documents, which include both Russian standards, namely GOST 32144-2013 [16], and international standards, such as EN 50160:2022 [17]. The above-mentioned standards limit only voltage waveform distortions; however, there also exists an international standard, IEEE 519-2014 [18], which limits distortions of both voltage and current [19].

The conventional method used in power quality assessment in terms of voltage and current waveform distortion is harmonic analysis. This method is based on representing a periodic signal by its Fourier series and computing its spectral components using the discrete Fourier transform (DFT). Harmonic analysis makes it possible to represent a complex signal as a sum of harmonic components, which, firstly, enables further calculations to find unknown components, and, secondly, allows the level of distortion to be quantified using the total harmonic distortion (THD) and the coefficients of individual harmonics [20,21]. Moreover, it is the harmonic analysis method that underlies most known methods for improving power quality, such as passive and active harmonic filters [22–24] or random frequency modulation algorithms [25].

However, despite its advantages, the harmonic analysis method also has a number of limitations that significantly affect the solution of modern problems in the field of power quality assessment [26]. Firstly, this method assumes strict periodicity of the signal over a given observation interval. However, in real power systems, such conditions are rare; non-stationary components often appear in power system signals, for example, during transient processes, which cannot be described using the DFT [27–29].

Secondly, the harmonic analysis method is not designed to detect and quantify interharmonics—components with frequencies that are not integer multiples of the fundamental frequency [19]. The occurrence of interharmonics can be caused by the presence of arc steelmaking furnaces, certain frequency converters, and other loads with fluctuating current consumption in the network [30]. The resulting spectral leakage effect and insufficient frequency resolution significantly complicate the task of accurately measuring interharmonics using harmonic analysis [31,32].

To address the above-mentioned drawbacks, various extensions of the DFT have been proposed. For example, the use of the generalized DFT to improve dynamic performance [33], the application of window functions to enhance measurement accuracy [32], or the use of the Stockwell transform for dealing with non-stationary signals [31]. Also, for example, in study [34], an identification method based on BP-NN is considered, a component of which is the DFT. This method makes it possible to accurately determine resonant frequencies and calculate motor parameters; however, it is not designed to form an accurate analytical description of the voltage or current waveform.

One of the promising approaches that makes it possible to eliminate the above-mentioned drawbacks is the use of approximation methods to describe the waveform [35,36]. Approximation methods have previously been used by researchers, in particular, to obtain standard voltage and current waveforms for various processes in an electric power system [37,38]. In the present study, the use of the spline interpolation method is proposed. Unlike harmonic analysis, which involves decomposing a signal into components, spline interpolation analytically describes the shape of a periodic non-sinusoidal signal by means of piecewise polynomial functions [39,40]. A key advantage of splines is the smoothness and continuity of the function itself and its first and second derivatives at the interpolation nodes, which not only ensures high approximation accuracy with a relatively small number of parameters, but also facilitates the subsequent solution of differential equations.

The spline interpolation method finds wide application in various fields of science and technology. Thus, this method is used in engineering geodesy for the analysis of acquired data [39,41]. In speech recognition technologies, spline interpolation enables the determination of emotional coloring [42]. In image processing, cubic and B-splines are used, enabling scaling, correction, and restoration of images [43].

Despite the application of spline interpolation in various fields, in the electric power engineering domain, this method is hardly ever used in its pure form, often serving as a supplement to already existing methods, such as the DFT. For instance, in [44], spline interpolation is used to extract the fundamental harmonic and further evaluate signal waveform distortion. In [45], the discrete Taylor–Fourier transform and O-splines are used for the analysis of fluctuating signals with varying frequency. Moreover, spline interpolation can be employed in signal preprocessing in order to simplify the subsequent application of the DFT [46,47].

In this paper, the authors propose a comparative analysis of two different approaches to describing periodic non-sinusoidal voltage and current signals: harmonic analysis, chosen due to its widespread use in industry and the availability of a regulatory framework, and spline interpolation, which has not previously been used as an independent method. The aim of the work is to quantitatively assess the accuracy of these methods when solving standard electric power engineering problems. Section 2 describes the theoretical foundations and research methodology, Section 3 presents the results of computer simulation of various electrical signals, Section 4 assesses the prospects of the spline interpolation method compared to harmonic analysis, and Section 5 presents the main conclusions of the study.

2. Materials and Methods

In the present study, a comparison was made between the harmonic analysis method and the spline interpolation method, which were used to analyze the waveform of periodic non-sinusoidal electrical signals, including the analysis of voltage and current waveforms at a given connection point.

The authors of the paper propose the application of the spline interpolation method, which enables the analysis of the waveform of periodic non-sinusoidal electrical signals by means of interpolating piecewise polynomial functions without sinusoidal decomposition of the signal.

The paper examines the use of piecewise polynomial functions of degree three, or cubic splines. A cubic spline consists of cubic segments. Each segment is defined on the interval between interpolation nodes and represents a polynomial of the third degree:

$$f_k(t) = a_k + b_k \cdot (t - t_{k-1}) + c_k \cdot (t - t_{k-1})^2 + d_k \cdot (t - t_{k-1})^3, \quad (1)$$

where $f_k(t)$ is the value of the function on the k-th segment at a given time t; a_k, b_k, c_k, and d_k are the polynomial coefficients on the considered k-th segment; t_{k-1} is the time value at the beginning of the k-th segment.

At $t = t_{k-1}$, function (1) takes the following form:

$$f_k(t_{k-1}) = a_k + b_k \cdot (t_{k-1} - t_{k-1}) + c_k \cdot (t_{k-1} - t_{k-1})^2 + d_k \cdot (t_{k-1} - t_{k-1})^3 = a_k, \quad (2)$$

that is, the value of the considered function at the interpolation node is equal to its value at the beginning of the segment and equals the constant term a_k.

The segments are joined at the interpolation nodes, ensuring the smoothness and continuity of the function, its first and second derivatives. For this purpose, at the inter-

polation nodes, the values of adjacent polynomials and their first and second derivatives must be equal:

$$\begin{cases} f_k(t_k) = f_{k+1}(t_k) \\ f_k\prime(t_k) = f_{k+1}\prime(t_k) \\ f_k''(t_k) = f_{k+1}''(t_k) \end{cases}. \quad (3)$$

Another condition for using spline interpolation is a specified distance between adjacent interpolation nodes. This distance is called the spline segment length and is denoted as h:

$$h = t_k - t_{k-1}. \quad (4)$$

By substituting (1) and (3) into (2), a system of linear equations with unknown coefficients b_k, c_k, and d_k is obtained:

$$\begin{cases} a_k + b_k \cdot h + c_k \cdot h^2 + d_k \cdot h^3 = a_{k+1} \\ b_k + 2 \cdot c_k \cdot h + 3 \cdot d_k \cdot h^2 = b_{k+1} \\ 2 \cdot c_k + 6 \cdot d_k \cdot h = 2 \cdot c_{k+1} \rightarrow c_k + 3 \cdot d_k \cdot h = c_{k+1} \end{cases}. \quad (5)$$

In the present study, it is assumed that, given the periodic nature of the signals under consideration, $f_n(t_n) = f_{n+1}(t_n) = f_1(t_0)$, where t_n is the time value at the end of the considered segment. Here, the observation interval ending at t_n may either equal the period of the fundamental frequency of the electrical signal or be an integer multiple of it, which makes it possible to analyze signals over longer time intervals and to take temporal variations into account, unlike the harmonic analysis method.

Thus, a system of $3n$ equations with $3n$ unknowns is formed, where n is the number of segments over the considered time interval. The system of equations is solved using matrix inversion. The obtained set of coefficients b_k, c_k, and d_k, together with the previously determined coefficients a_k, forms a set of cubic segments of the spline (1), which analytically describe the considered time interval of the electrical signal.

To verify the effectiveness of the spline interpolation method and to perform a comparative analysis of the two above-mentioned methods, computer simulation of a simple electric power system with two types of connected load, linear and nonlinear, was carried out using NI Multisim 14.2 (Multisim Education Edition, application version 14.2.0, build 14.20.49240, database version 14.1.a). The nonlinear load is external to the consumer under consideration and is represented by a three-phase Larionov rectifier with a connected resistive load and an inductive impedance required for current smoothing, represented by a coil with an inductance of 0.1 mH. The connection of the nonlinear load contributes to the appearance of harmonic components of the supply voltage at the point of common coupling of the linear load. The type of linear load depends on the simulation scheme. Within Scheme A, the linear load is represented by a simple equivalent circuit of a power transmission line and parallel-connected resistive-inductive and resistive consumers (Figure 1). Within Scheme B, a capacitor bank (CB) is connected at the point of common coupling of the existing linear consumer, represented by non-ideal capacitors connected in a star configuration (Figure 2).

The source voltage parameters and the line resistance R_{line} and inductance L_{line} are specified and remain unchanged. The simulation is carried out at a line voltage of 6.3 kV. The linear load parameters are specified separately for each scheme.

The parameters of the Larionov rectifier load on the direct current (DC) side (the resistance of the nonlinear load R_n), which are necessary for varying the degree of supply voltage distortion, are presented in Table 1. The power of the nonlinear load directly affects the total harmonic distortion THD_U.

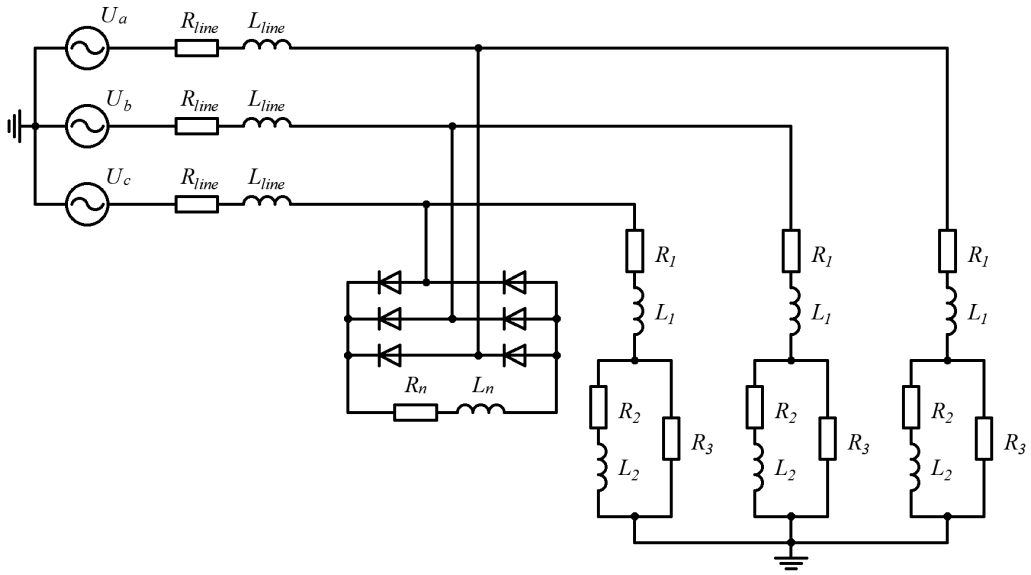


Figure 1. Equivalent circuit of the electric power system (Scheme A) [compiled by the authors].

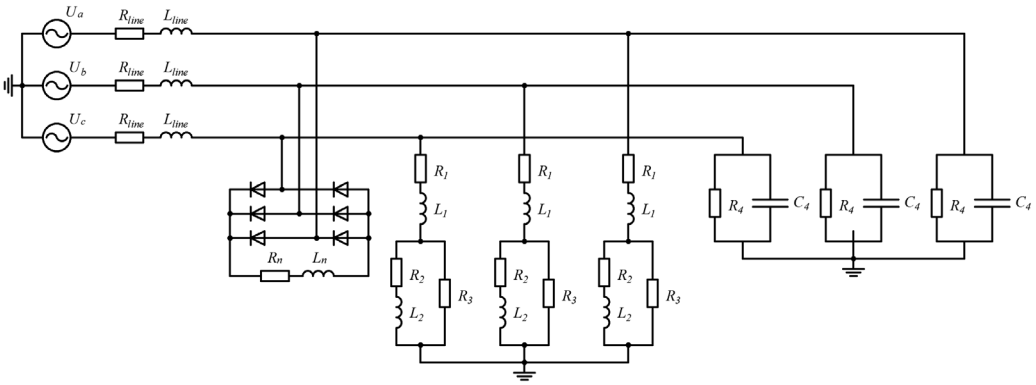


Figure 2. Equivalent circuit of the electric power system with a CB (Scheme B) [compiled by the authors].

Table 1. Rectifier load parameters [compiled by the authors].

No.	1	2	3	4	5	6	7	8	9	10
R_n, Ω	50	45	40	35	30	25	22	19	16	13

In the computer simulation for Scheme A (Figure 1), the following parameters presented in Table 2 were used. These parameters correspond to the load of various workshops of a metallurgical plant and make it possible to evaluate how various load power parameters affect the analysis accuracy.

Table 2. Parameters of equivalent circuit A [compiled by the authors].

Scheme No.	L_1, mH	R_1, Ω	L_2, mH	R_2, Ω	R_3, Ω
1	0.150	0.072	42.813	17.296	39.690
2	0.260	0.126	32.076	13.450	132.300
3	0.260	0.126	320.761	134.502	496.125

In the computer simulation for Scheme B, the parameters of one of the equivalent circuits of Scheme A and the parameters of the CB presented in Table 3 were used.

Table 3. Parameters of equivalent circuit B [compiled by the authors].

Scheme No.	Scheme A No.	CB Mode	C_4, mF	R_4, MΩ
1	1	Compensation	0.088	113.354
2	1	Overcompensation	0.120	83.127
3	1	Undercompensation	0.056	178.128
4	3	Undercompensation	0.002	6234.491

In the simulation of Scheme A, the following data were obtained from one of the phases:

1. Phase voltage of the network at the connection point, $u_0(t)$;
2. Line current flowing through R_1 and L_1, $i_1(t)$;
3. Current of the resistive-inductive load flowing through R_2 and L_2, $i_2(t)$;
4. Current of the resistive load flowing through R_3, $i_3(t)$.

The instantaneous values of the current flowing through the resistors were obtained by recording the voltage waveform across the resistor and subsequently applying Ohm's law.

In the simulation of Scheme B, the following data were obtained from one of the phases:

1. Phase voltage of the network at the connection point, $u_0(t)$;
2. Capacitor current flowing through C4, $\mathrm{i}_4(\mathrm{t})$.

The instantaneous values of the current flowing through the capacitor were obtained by recording the voltage waveform across an auxiliary resistor connected in series and having a low resistance (1 μΩ), and subsequently applying Ohm's law.

The obtained sets of instantaneous voltage and current values are represented as discrete time series with a signal sampling period specified during the simulation.

To analyze periodic non-sinusoidal electrical signals, it is necessary to analytically describe the available discrete time series, for which purpose the methods of harmonic analysis and spline interpolation are applied. In the present study, the instantaneous values of the phase voltage at the connection point are described; then, by solving differential equations, analytical descriptions of the considered instantaneous current values are obtained.

To derive the differential equations, the single-line equivalent circuits presented in Figure 3 were used.

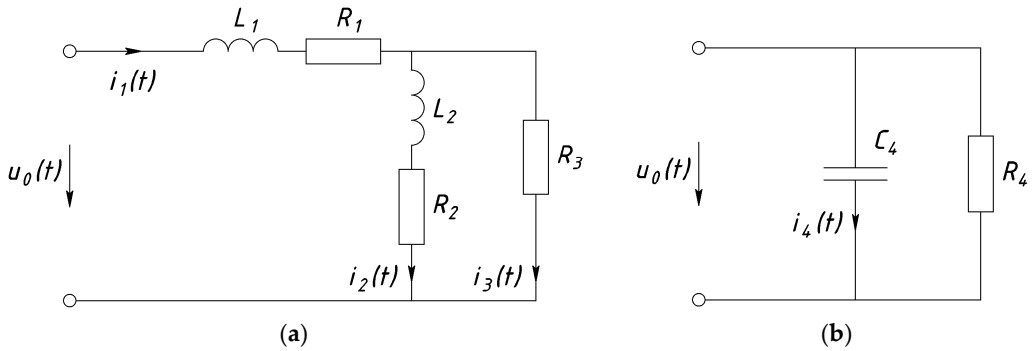


Figure 3. (**a**) Single-line equivalent circuits for Scheme A; (**b**) Single-line equivalent circuits for Scheme B [compiled by the authors].

The system of differential equations for Scheme A:

$$\begin{cases} u_0(t) = i_1(t)\cdot R_1 + L_1\cdot\frac{di_1(t)}{dt} + i_2(t)\cdot R_2 + L_2\cdot\frac{di_2(t)}{dt} \\ u_0(t) = i_1(t)\cdot R_1 + L_1\cdot\frac{di_1(t)}{dt} + i_3(t)\cdot R_3 \\ i_1(t) = i_2(t) + i_3(t) \end{cases}. \quad (6)$$

The system of differential equations for Scheme B:

$$\begin{cases} u_0(t) = u_{C4}(t) = u_{R4}(t) \\ i_4(t) = C_4\cdot\frac{du_{C4}(t)}{dt} \end{cases}. \quad (7)$$

The analytical descriptions of the instantaneous value of the supply voltage at the connection point, obtained using harmonic analysis and spline interpolation, are substituted into the systems of differential equations.

The solution of differential equations when using the harmonic analysis method is based on the symbolic method. The values of amplitudes and initial phases for each frequency that is an integer multiple of the fundamental frequency, up to the 50th order, obtained by means of the Fourier analysis built into the Multisim software, are used to form the complex amplitudes of each harmonic. The conversion into analytical form is carried out using Euler's formula as follows:

$$\dot{A} = Ae^{j\alpha} \leftrightarrow A\cdot\sin(\omega t + \alpha). \quad (8)$$

Differential Equations (6) and (7), transformed for solution by the symbolic method taking into account the component equations, are as follows:

System of equations for Scheme A:

$$\begin{cases} \dot{U}_{m0} = \dot{I}_{m1}\cdot R_1 + \dot{I}_{m1}\cdot\left(e^{j\frac{\pi}{2}}\cdot\omega L_1\right) + \dot{I}_{m2}\cdot R_2 + \dot{I}_{m2}\cdot\left(e^{j\frac{\pi}{2}}\cdot\omega L_2\right) \\ \dot{U}_{m0} = \dot{I}_{m1}\cdot R_1 + \dot{I}_{m1}\cdot\left(e^{j\frac{\pi}{2}}\cdot\omega L_1\right) + \dot{I}_{m3}\cdot R_3 \\ \dot{I}_{m1} = \dot{I}_{m2} + \dot{I}_{m3} \end{cases}. \quad (9)$$

System of equations for Scheme B:

$$\begin{cases} \dot{U}_{m0} = \dot{U}_{mC4} = \dot{U}_{mR4} \\ \dot{I}_{m4} = \frac{\dot{U}_{mC4}}{\frac{1}{\omega C_4}\cdot e^{j\cdot(-\frac{\pi}{2})}} = \dot{U}_{mC4}\cdot\omega C_4\cdot e^{j\frac{\pi}{2}} \end{cases}. \quad (10)$$

The solution of differential equations when using the spline interpolation method is carried out by means of the operational method. In order to obtain a particular solution of the equations, the following condition is taken into account:

$$f_1(t) = f_{N+1}(t), \quad (11)$$

where N is the total number of spline segments over the considered interval.

In order for this limitation not to affect the accuracy of the results in the presence of interharmonics in the network, it is necessary to extend the length of the considered interval when solving differential equations, and then discard the extreme values, as will be shown below.

The original cubic spline (1) is transformed into its Laplace image by means of the Laplace transform for solution by the operational method. The transformation process is presented in Appendix A.

$$F_k(p) = \frac{a_k}{p} + \frac{b_k}{p^2}\cdot e^{-t_{k-1}p} + \frac{2c_k}{p^3}\cdot e^{-t_{k-1}p} + \frac{6d_k}{p^4}\cdot e^{-t_{k-1}p}. \quad (12)$$

Differential Equations (6) and (7), transformed for solution by the operational method, are as follows:

System of equations for Scheme A:

$$\begin{cases} U_{m0}(p) = I_{m1}(p)\cdot R_1 + I_{m1}\cdot pL_1 - i_1(0)\cdot L_1 + I_{m2}(p)\cdot R_2 + I_{m2}\cdot pL_2 - i_2(0)\cdot L_2 \\ U_{m0}(p) = I_{m1}(p)\cdot R_1 + I_{m1}\cdot pL_1 - i_1(0)\cdot L_1 + I_{m3}(p)\cdot R_3 \\ I_{m1}(p) = I_{m2}(p) + I_{m3}(p) \end{cases}. \quad (13)$$

System of equations for Scheme B:

$$\begin{cases} U_{m0}(p) = U_{mC4}(p) = U_{mR4}(p) \\ U_{mC4}(p) = I_{m4}(p)\cdot\frac{1}{pC_4} + \frac{u_{C4}(0)}{p} \rightarrow I_{m4}(p) = \left(U_{mC4}(p) - \frac{u_{C4}(0)}{p}\right)\cdot pC_4 \end{cases}. \quad (14)$$

The obtained particular solution of the differential equation represents a set of coefficients describing the calculated currents for each cubic segment of the spline over a given interval.

The comparison of the methods is primarily carried out by means of an integral deviation assessment, namely, by calculating the integral of absolute error (IAE) in discrete form [48], according to the following formula:

$$\mathrm{IAE} = \sum_{l=0}^{N-1} |e(t_l)|\Delta t, \quad (15)$$

where l is the index number of a point, N is the number of points on the considered interval of the function, $e(t_l)$ is the difference between the original simulation waveform and the value obtained using one of the methods for analytical description, and Δt is the sampling period.

The IAE is reduced to a dimensionless form to ensure correct comparison of different signals. The normalized integral of absolute error (NIAE) is obtained by dividing the IAE by the area under the curve of the absolute value of the original signal (voltage or current):

$$\mathrm{NIAE} = \frac{\mathrm{IAE}}{\sum_{l=0}^{N-1} |x(t_l)|\Delta t} \quad (16)$$

where $x(t_l)$ is the original instantaneous voltage or current value at time t_l.

3. Results

As a result of computer simulation, instantaneous voltage values were obtained, presented as time series with a sampling period of 12.5 µs. Based on Ohm's law and the instantaneous voltage values across the resistors, the instantaneous values of the currents flowing in the branches were calculated. The obtained voltage and current time series are considered to be the original instantaneous values. In the subsequent analysis, a time interval of 0.4 s was considered, i.e., comprising two periods of the fundamental frequency.

Since the previously mentioned international standards regulate the analysis of non-sinusoidal voltages up to the 50th harmonic, the waveform analysis will be limited to this number of harmonics. This is due to the intended further use of the research results for

industrial consumers, in whose case power quality monitoring instruments are most often designed for analysis up to the 50th harmonic. Using the built-in Fourier analysis tool, sets of amplitude and initial phase values for harmonics from the 1st to the 50th, as well as the value of the DC component of the phase voltage and the value of THD_U, were obtained. By solving differential Equations (9) and (10), depending on the scheme under consideration, sets of instantaneous current values were obtained. In this paper, the instantaneous line current values for Scheme A and the instantaneous capacitor current values for Scheme B are considered.

The obtained sets were transformed into harmonics of the corresponding frequencies, which were then summed to obtain the reconstructed instantaneous voltage and current values, which are hereinafter considered as obtained by the harmonic analysis method.

The choice of the spline segment length is made taking into account the Nyquist–Shannon theorem [49]. The minimum required signal sampling period for the analysis of the 50th harmonic is 0.2 ms.

Consequently, a set of instantaneous phase voltage values with a sampling period of 0.2 ms is guaranteed to be obtained, and this set of values is used as interpolation nodes. A set of coefficients for cubic splines that analytically describe the instantaneous voltage value was obtained. The obtained analytical descriptions were substituted into differential Equations (13) and (14); in the course of solving the equations, sets of coefficients corresponding to the splines of the instantaneous capacitor current value were obtained. Hereinafter, the instantaneous voltage and current values are considered to be obtained by spline interpolation.

To assess the accuracy and perform a comparative analysis of the methods, the absolute deviation of the discrete values obtained by harmonic analysis and spline interpolation is calculated relative to the original values:

$$e_{uh}(t_l) = u(t_l) - u_h(t_l), \tag{17}$$

$$e_{us}(t_l) = u(t_l) - u_s(t_l), \tag{18}$$

where $u(t_l)$ is the original instantaneous voltage value at time t_l, V; $u_h(t_l)$ is the instantaneous voltage value obtained by harmonic analysis, V; $u_s(t_l)$ is the instantaneous voltage value obtained by spline interpolation, V; $e_{uh}(t_l)$ is the absolute deviation of the instantaneous voltage value obtained by harmonic analysis at time t_l, V; $e_{us}(t_l)$ is the absolute deviation of the instantaneous voltage value obtained by spline interpolation at time t_l, V;

$$e_{ih}(t_l) = i(t_l) - i_h(t_l), \tag{19}$$

$$e_{is}(t_l) = i(t_l) - i_s(t_l), \tag{20}$$

where $i(t_l)$ is the original instantaneous current value at time t_l, A; $i_h(t_l)$ is the instantaneous current value obtained by harmonic analysis, A; $i_s(t_l)$ is the instantaneous current value obtained by spline interpolation, A; $e_{ih}(t_l)$ is the absolute deviation of the instantaneous current value obtained by harmonic analysis at time t_l, A; $e_{is}(t_l)$ is the absolute deviation of the instantaneous current value obtained by spline interpolation at time t_l, A.

By substituting the obtained absolute deviation values into (15) and (16) for each set of values of each scheme, the NIAE was calculated. The results are grouped according to the schemes; when visualizing the obtained results, the THD_U values, which depend on the rectifier load, and the NIAE values are plotted on the graphs.

The results of calculating the instantaneous values of the phase voltage at the connection point and the instantaneous values of the line current for Schemes A1–A3 are presented in Figures 4 and 5. In addition, the calculation results for these and other schemes are presented in tabular form in Appendix B.

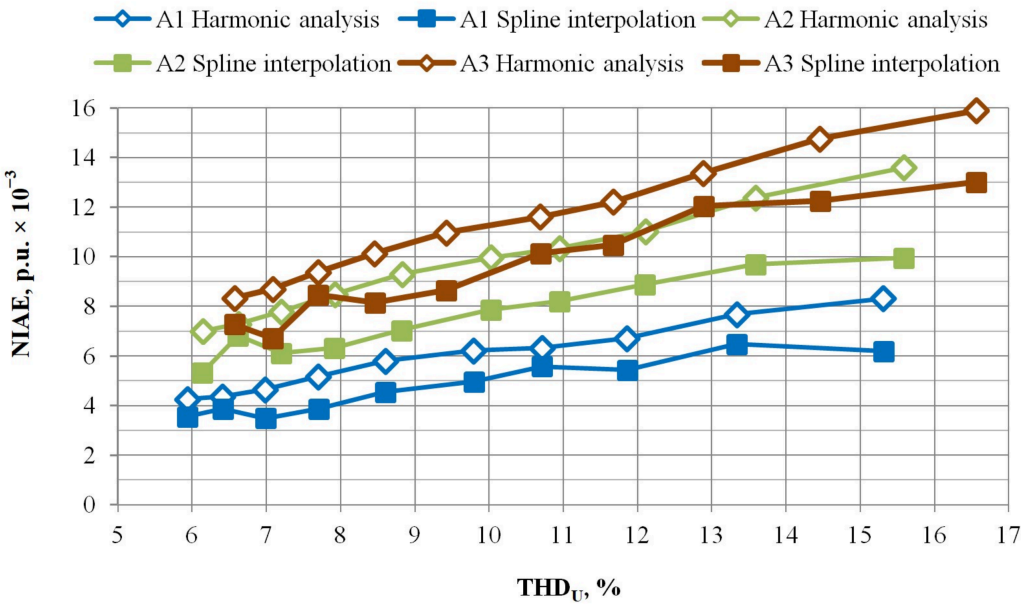


Figure 4. NIAE for the instantaneous voltage value of Schemes A1, A2, and A3 [compiled by the authors].

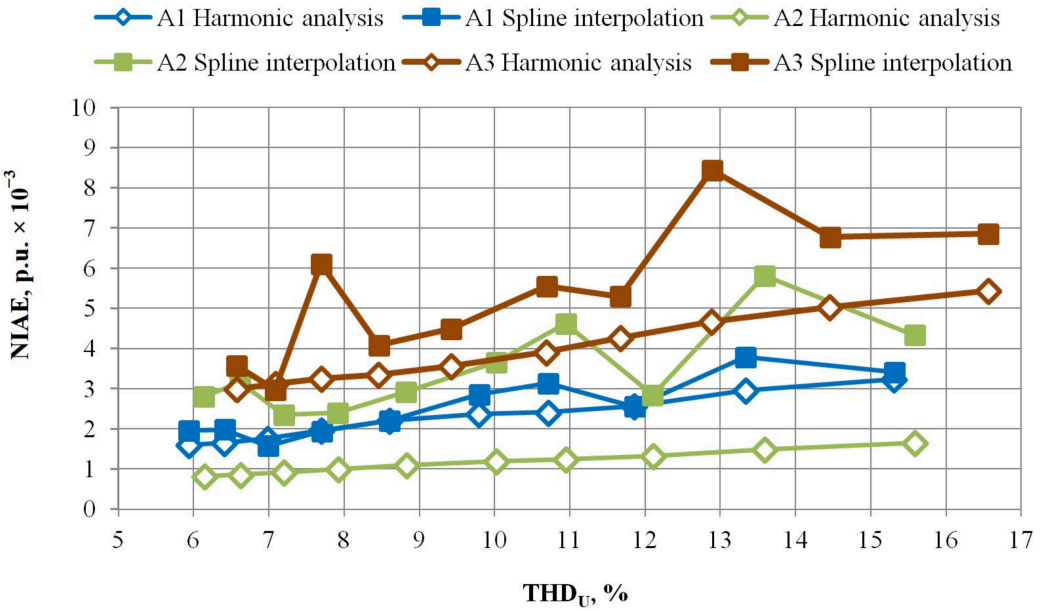


Figure 5. NIAE for the instantaneous current value of Schemes A1, A2, and A3 [compiled by the authors].

The results of calculating the instantaneous values of the phase voltage at the connection point and the instantaneous values of the capacitor current for Schemes B1–B3 are presented in Figures 6 and 7.

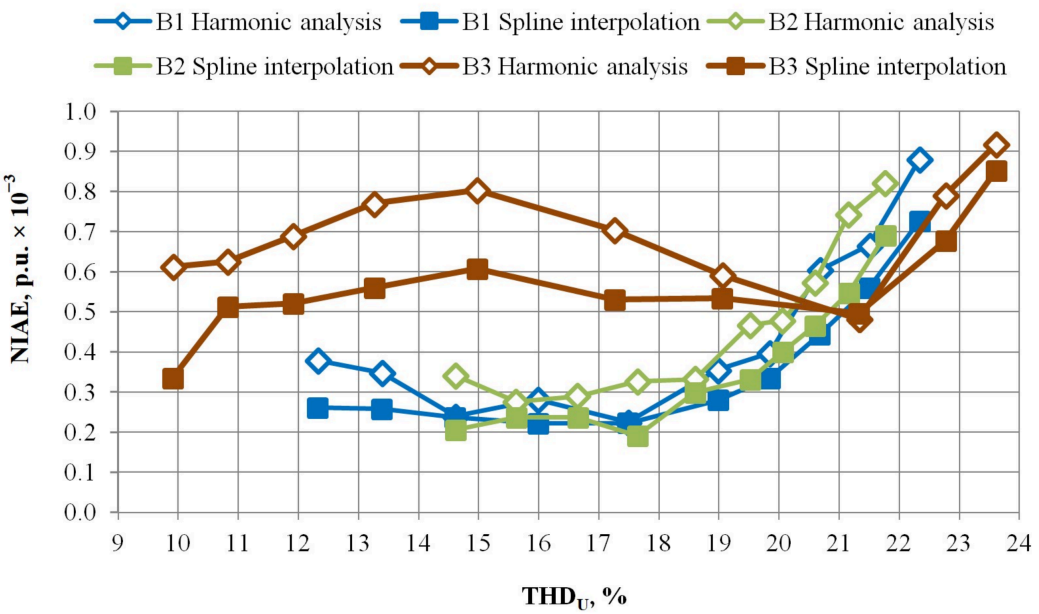


Figure 6. NIAE for the instantaneous voltage value of Schemes B1, B2, and B3 [compiled by the authors].

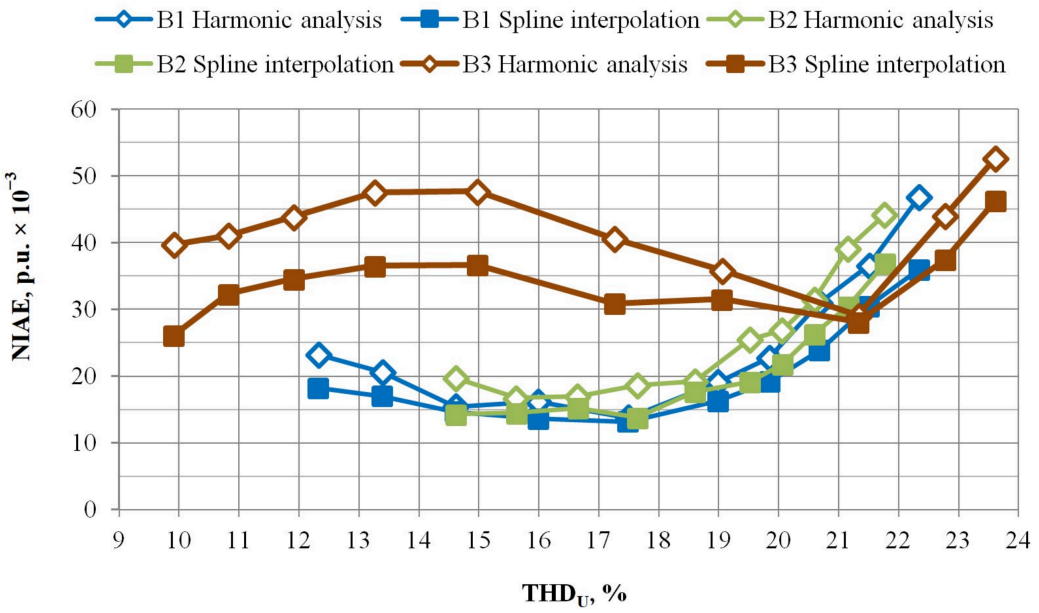


Figure 7. NIAE for the instantaneous current value of Schemes B1, B2, and B3 [compiled by the authors].

Scheme B4, which represents the connection of a low-power capacitor bank to Scheme A3, where the linear load is significantly lower in power compared to the other Scheme A variants, is considered separately. Furthermore, to confirm the possibility of using spline interpolation in the presence of interharmonics, a voltage source with an amplitude equal to 3% of the fundamental frequency amplitude and a frequency of 67 Hz was connected to Scheme B4, which is typical of interharmonics generated by arc furnaces. This scheme is designated as Scheme B5; the calculated NIAE values for both schemes are presented in Figures 8 and 9.

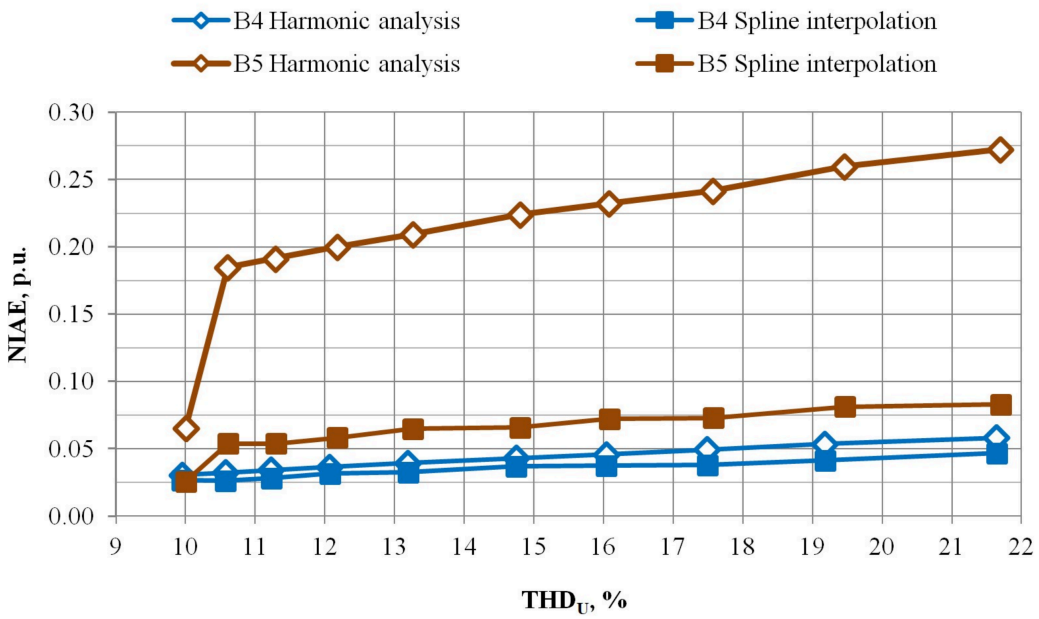


Figure 8. NIAE for the instantaneous voltage value of Schemes B4 and B5 [compiled by the authors].

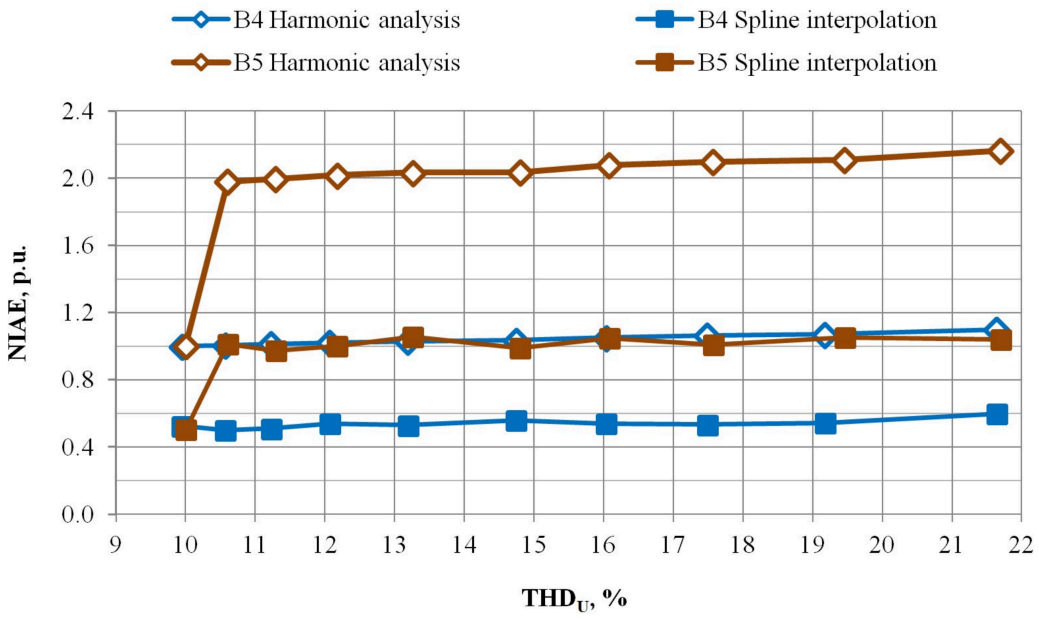


Figure 9. NIAE for the instantaneous capacitor current value of Schemes B4 and B5 [compiled by the authors].

4. Discussion

Thus, the hypothesis that the spline interpolation method can be applied for the analytical description of voltage and current waveforms has been confirmed. When using the spline interpolation method, it is possible to solve the main problems of electric power engineering, in particular, finding unknown currents in the network; moreover, as can be seen from the presented graphs, the deviation of instantaneous current values occurs within the same order of magnitude for both approaches. Thus, the spline interpolation method can be used instead of harmonic analysis in cases where accurate analytical description is required. The possibility of using the spline interpolation method in the presence of interharmonics in the network has also been confirmed.

Moreover, the NIAE for the supply voltage at the point of connection when using the spline interpolation method always takes smaller values than when using harmonic analysis; that is, for measured, rather than calculated, values, the spline interpolation method is more accurate.

Attention should also be paid to the results of Schemes B1–B3, namely, to the NIAE for the instantaneous capacitor current values (Figure 7). It can be observed that the waveform of the capacitor current obtained by spline interpolation is more accurate than that obtained by harmonic analysis. This is particularly important in view of the special danger of harmonic distortion for capacitors, as mentioned earlier.

In this regard, special attention should be paid to Scheme B4, since the NIAE values for the supply voltage waveforms take much larger values than in other cases. This is due to the waveform shape: the frequency of the distortion in the grid exceeds the frequency of the adopted 50th harmonic (in the case of harmonic analysis), and the sampling interval used for the grid distortion is shorter than the adopted spline segment length. For clarity, Figure 10 shows the voltage waveforms for Scheme A3 and for Scheme B4, which represents Scheme A3 with a low-power CB connected to it, at a DC-side resistance of 30 Ω.

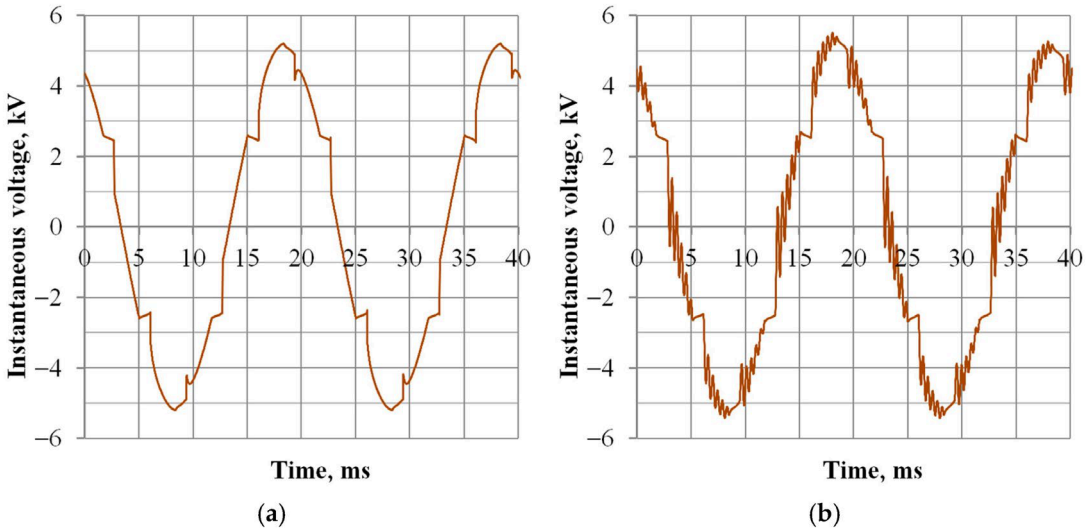


Figure 10. (**a**) Instantaneous voltage waveform at the connection point at a DC-side resistance of 30 Ω for Scheme A3; (**b**) Instantaneous voltage waveform at the connection point at a DC-side resistance of 30 Ω for Scheme B4 [compiled by the authors].

Let us consider separately the voltage waveform for Scheme B5 at a DC-side resistance of 30 Ω. For greater clarity, Figure 11 shows the signal over 0.1 s, as the effect of the interharmonic on the waveform is more clearly visible in this case. However, all calculations were performed in the same way as for the other schemes, over an interval of 0.4 s, to ensure comparability of values.

If attention is paid to Figure 9, it can be seen that the NIAE value for the capacitor current obtained by harmonic analysis exceeds the NIAE of spline interpolation by almost a factor of two, although the order of values remains within the same order of magnitude. A comparison is made between the actual waveform of the current curves reconstructed after harmonic analysis and spline interpolation and the original waveform. The original current waveform was obtained by applying Ohm's law to the simulated voltage signal across the auxiliary resistor. Figure 12 shows the capacitor current waveforms over two periods (40 ms) for Scheme B4 at a DC-side resistance of 30 Ω. Figure 13 similarly shows the current waveforms for Scheme B5 at a DC-side resistance of 30 Ω. To obtain the capacitor currents in the presence of interharmonics, the differential equations were solved taking

into account (11) over a longer interval, and then the extreme values distorted due to the inaccuracy of the periodicity condition were discarded.

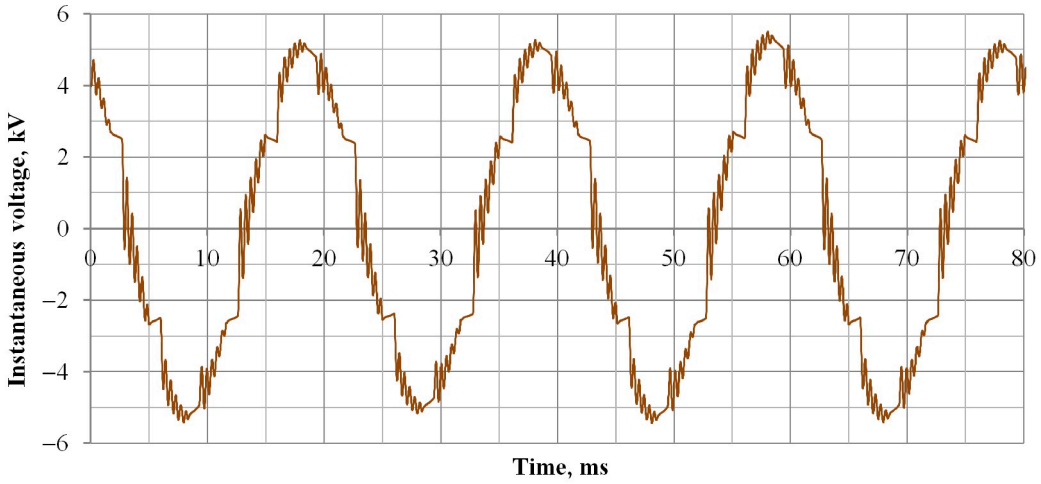


Figure 11. Instantaneous voltage waveform at the connection point at a DC-side resistance of 30 Ω for Scheme B5 [compiled by the authors].

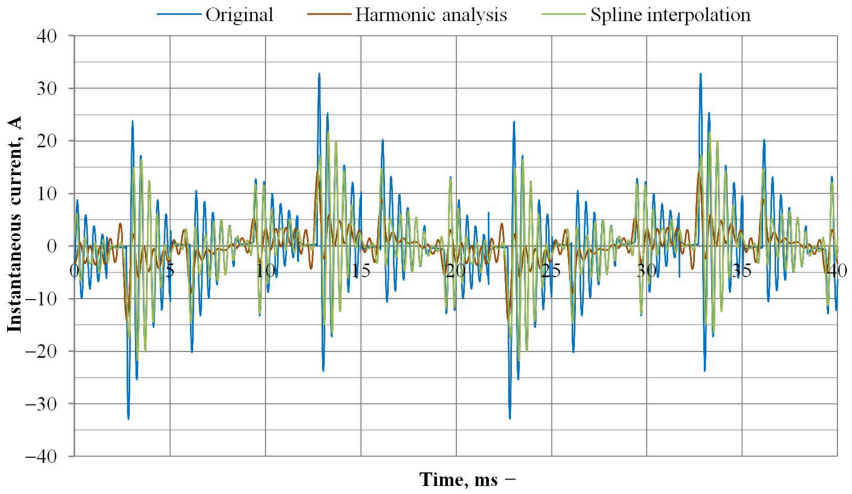


Figure 12. Instantaneous capacitor current waveform at a DC-side resistance of 30 Ω for Scheme B4 [compiled by the authors].

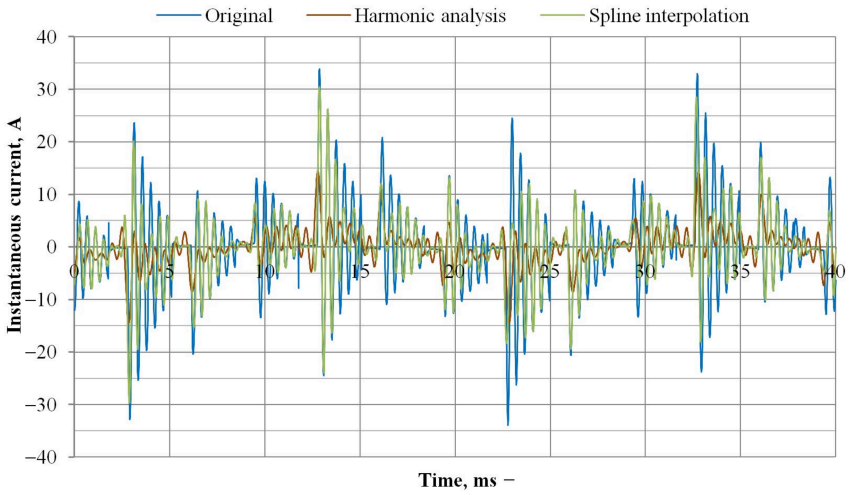


Figure 13. Instantaneous capacitor current waveform at a DC-side resistance of 30 Ω for Scheme B5 [compiled by the authors].

As can be seen, the current waveforms obtained by harmonic analysis and by spline interpolation differ significantly from the original current waveform. Special attention should be paid to the peak values reached by the instantaneous current, since CBs are sensitive to the exceedance of allowable current values. Figures 14 and 15 show the graphs of the magnitudes of the maximum current values through the capacitor for Schemes B4 and B5.

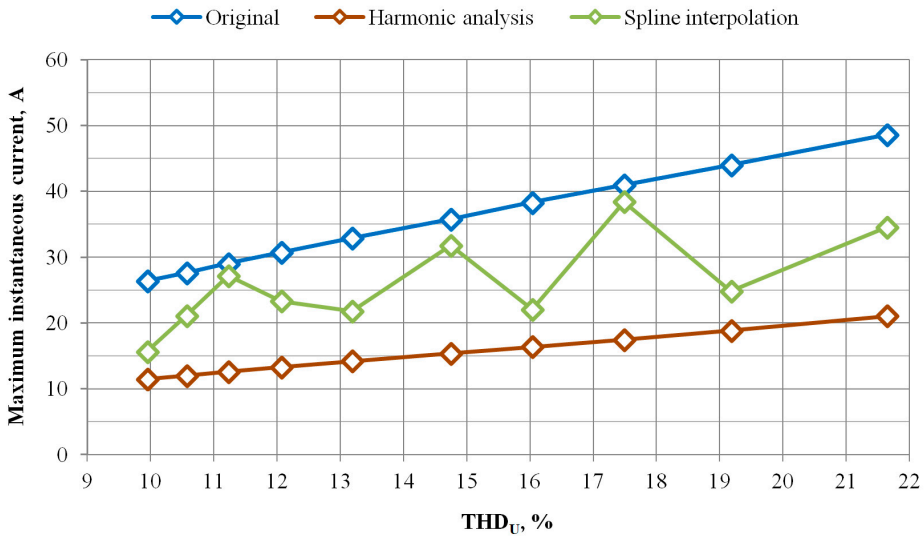


Figure 14. Maximum absolute value of the instantaneous capacitor current for Scheme B4 [compiled by the authors].

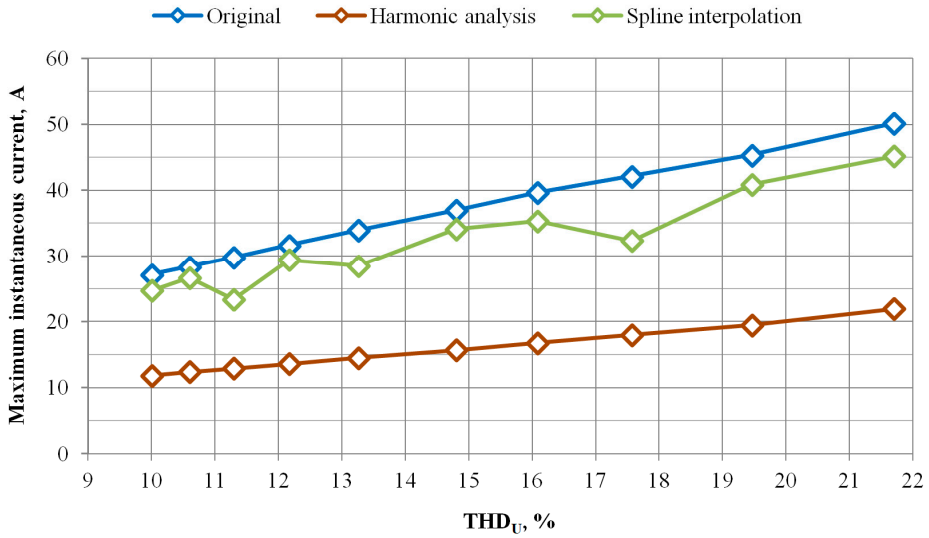


Figure 15. Maximum absolute value of the instantaneous capacitor current for Scheme B5 [compiled by the authors].

Thus, for Schemes B4 and B5, the values obtained by harmonic analysis are approximately 2.32 times smaller than the original maximum instantaneous current values. The values obtained using spline interpolation are on average 1.40 times smaller than the original values for Scheme B4, and 1.14 times smaller than the original values for Scheme B5.

For Schemes B4 and B5, in addition to calculating NIAE, when comparing different methods, the values of root mean square error (RMSE), maximum error, and mean relative error are also compared. The calculation results are presented in Tables 4 and 5.

Table 4. Values of RMSE, maximum error, and mean relative error for the capacitor current for Scheme B4 [compiled by the authors].

No.	THD_U, %	RMSE for Harmonic Analysis, A	RMSE for Spline Interpolation, A	Max. Error for Harmonic Analysis, A	Max. Error for Spline Interpolation, A	Mean Relative Error for Harmonic Analysis	Mean Relative Error for Spline Interpolation
1	9.94	5.74	3.52	17.14	15.40	4.58	2.44
2	10.57	6.03	3.16	18.01	10.33	5.46	2.44
3	11.23	6.35	3.33	19.00	10.58	3.45	2.79
4	12.07	6.74	4.32	20.22	18.71	3.47	2.89
5	13.19	7.24	4.16	21.79	17.01	4.08	2.88
6	14.74	7.91	4.71	23.86	19.89	3.27	2.27
7	16.04	8.39	5.13	25.73	22.81	3.71	2.59
8	17.49	8.96	4.85	27.69	15.33	4.49	3.25
9	19.17	9.64	5.96	29.94	26.83	3.69	1.89
10	21.64	10.36	7.12	33.30	29.78	5.04	3.09

Table 5. Values of RMSE, maximum error, and mean relative error for the capacitor current for Scheme B5 [compiled by the authors].

No.	THDU, %	RMSE for Harmonic Analysis, A	RMSE for Spline Interpolation, A	Max. Error for Harmonic Analysis, A	Max. Error for Spline Interpolation, A	Mean Relative Error for Harmonic Analysis	Mean Relative Error for Spline Interpolation
1	9.94	6.08	3.25	24.72	16.34	4.18	2.55
2	10.57	6.46	3.59	26.06	16.90	3.34	2.69
3	11.23	6.80	3.59	27.44	17.68	3.02	2.33
4	12.07	7.22	3.71	29.02	18.06	2.44	1.88
5	13.19	7.73	4.36	31.05	21.39	2.50	2.04
6	14.74	8.44	4.35	33.80	21.43	6.42	2.55
7	16.04	8.95	5.01	36.07	24.48	3.23	2.59
8	17.49	9.54	5.08	39.02	24.94	3.24	2.30
9	19.17	10.31	5.78	41.98	27.18	3.36	2.52
10	21.64	11.16	5.88	45.42	28.16	3.61	2.37

Therefore, spline interpolation enables more accurate determination of peak current values, which is important for the selection and performance assessment of CBs.

5. Conclusions

The authors conducted a comparative analysis of the harmonic analysis method, which is the most widely used method in industry, and the spline interpolation method, which has not previously been used as an independent method for analyzing the waveform of an electrical signal.

The conducted study shows that the spline interpolation method is a viable method for the analysis of periodic non-sinusoidal voltages and currents. The obtained results show that, similarly to the harmonic analysis method, it is possible to derive analytical descriptions of voltage and current waveforms using spline interpolation. Moreover, an additional advantage of spline interpolation is the ability to derive a more accurate analytical description of signals containing interharmonics, in contrast to the classical DFT.

The use of cubic splines made it possible to achieve high waveform reproduction accuracy, comparable to or even surpassing the accuracy of harmonic analysis. In particular, the accuracy of spline interpolation in reproducing the waveform of the original supply voltage at the connection point exceeds the accuracy of harmonic analysis. It should be noted that, in this paper, harmonic analysis was limited to the 50th harmonic, which, as mentioned above, is dictated by international standards. However, where power quality

monitoring instruments allow a larger number of harmonics to be analyzed, one can both increase the number of harmonics and proportionally reduce the spline segment length, thereby improving the accuracy of both methods.

An important advantage of spline interpolation is also its higher accuracy in reproducing the waveform of the current flowing through the capacitor compared with harmonic analysis in cases where, in accordance with the Nyquist–Shannon sampling theorem, the spline segment length corresponds to the sampling period required for the analysis of harmonics of a given order. Thus, the method can contribute to a more accurate assessment of peak current values and, as a consequence, to a more accurate assessment of the risk of capacitor-bank failure.

Thus, in the present study, it has been demonstrated that spline interpolation is a viable method for analyzing voltage and current waveforms in the network. This method has the potential for implementation in power quality monitoring and metering systems and in the field of electrical equipment diagnostics. Further research will be aimed at developing specific algorithms for applying the spline interpolation method in these fields, as well as at developing an approach to the selection of filter-compensating devices using spline interpolation in the metallurgical industry.

Author Contributions: Conceptualization, Y.S. and Y.K.; methodology, O.B. and Y.K.; validation, Y.S., O.B. and Y.K.; formal analysis, Y.K.; investigation, O.B. and Y.K.; resources, Y.S.; data curation, O.B.; writing—original draft preparation, O.B. and Y.K.; writing—review and editing, Y.S. and O.B.; visualization, Y.K.; supervision, Y.S.; project administration, Y.S. All authors have read and agreed to the published version of the manuscript.

Funding: This research received no external funding.

Institutional Review Board Statement: Not applicable.

Informed Consent Statement: Not applicable.

Data Availability Statement: The original contributions presented in this study are included in the article. Further inquiries can be directed to the corresponding author.

Acknowledgments: During the preparation of this manuscript, the authors used DeepSeek-V4-Flash-0731 for the purposes of language editing (grammar correction) in limited sections of the manuscript. The authors have reviewed and edited the output and take full responsibility for the content of this publication.

Conflicts of Interest: The authors declare no conflicts of interest.

Abbreviations

The following abbreviations are used in this manuscript:

IEEE	Institute of Electrical and Electronics Engineers
DFT	Discrete Fourier Transform
THD	Total Harmonic Distortion
CB	Capacitor Bank
DC	Direct Current
IAE	Integral of Absolute Error
NIAE	Normalized Integral of Absolute Error
RMSE	Root Mean Square Error

Appendix A

Original function:

$$f_k(t) = a_k + b_k \cdot (t - t_{k-1}) + c_k \cdot (t - t_{k-1})^2 + d_k \cdot (t - t_{k-1})^3. \quad \text{(A1)}$$

A tabular Laplace transform is used:

$$F(t^n) = \frac{n!}{p^{n+1}}, \tag{A2}$$

$$a_k \to a_k \cdot \frac{0!}{p^{0+1}} = \frac{a_k}{p}, \tag{A3}$$

$$b_k \cdot t \to b_k \cdot \frac{1!}{p^{1+1}} = \frac{b_k}{p^2}, \tag{A4}$$

$$c_k \cdot t^2 \to c_k \cdot \frac{2!}{p^{2+1}} = \frac{2c_k}{p^3}, \tag{A5}$$

$$d_k \cdot t^3 \to d_k \cdot \frac{3!}{p^{3+1}} = \frac{6d_k}{p^4}, \tag{A6}$$

Since the formula uses $t - t_{k-1}$ it is necessary to apply the delay theorem:

$$F(f(t - t_{k-1}) \cdot \eta(t - t_{k-1})) = F(p) \cdot e^{-pt_{k-1}}, \tag{A7}$$

$$b_k \cdot (t - t_{k-1}) \to \frac{b_k}{p^2} \cdot e^{-t_{k-1}p}, \tag{A8}$$

$$c_k \cdot (t - t_{k-1})^2 \to \frac{2c_k}{p^3} \cdot e^{-t_{k-1}p}, \tag{A9}$$

$$d_k \cdot (t - t_{k-1})^3 \to \frac{6d_k}{p^4} \cdot e^{-t_{k-1}p} \tag{A10}$$

Thus, the Laplace transform of the original function (A1) is given by the following formula:

$$F_k(p) = \frac{a_k}{p} + \frac{b_k}{p^2} \cdot e^{-t_{k-1}p} + \frac{2c_k}{p^3} \cdot e^{-t_{k-1}p} + \frac{6d_k}{p^4} \cdot e^{-t_{k-1}p} \tag{A11}$$

Appendix B

Table A1. NIAE for the instantaneous voltage or current value of Scheme A1 [compiled by the authors].

No.	THD_U, %	NIAE of Voltage, Harmonic Analysis, p.u. $\times 10^{-3}$	NIAE of Voltage, Spline Interpolation, p.u. $\times 10^{-3}$	NIAE of Current, Harmonic Analysis, p.u. $\times 10^{-3}$	NIAE of Current, Spline Interpolation, p.u. $\times 10^{-3}$
1	5.93	4.27	3.55	1.61	1.96
2	6.41	4.38	3.87	1.65	1.98
3	6.99	4.66	3.49	1.76	1.58
4	7.70	5.18	3.87	1.97	1.94
5	8.60	5.81	4.54	2.21	2.20
6	9.79	6.23	4.96	2.37	2.86
7	10.71	6.34	5.58	2.42	3.14
8	11.86	6.72	5.43	2.57	2.56
9	13.33	7.68	6.48	2.96	3.79
10	15.31	8.32	6.20	3.23	3.42

Table A2. NIAE for the instantaneous voltage or current value of Scheme A2 [compiled by the authors].

No.	THD_U, %	NIAE of Voltage, Harmonic Analysis, p.u. $\times 10^{-3}$	NIAE of Voltage, Spline Interpolation, p.u. $\times 10^{-3}$	NIAE of Current, Harmonic Analysis, p.u. $\times 10^{-3}$	NIAE of Current, Spline Interpolation, p.u. $\times 10^{-3}$
1	6.14	7.00	5.34	0.83	2.81
2	6.62	7.29	6.82	0.86	3.16
3	7.20	7.79	6.13	0.92	2.36
4	7.92	8.49	6.33	1.00	2.41
5	8.82	9.30	7.05	1.10	2.92
6	10.02	9.96	7.87	1.20	3.66
7	10.95	10.34	8.21	1.24	4.62
8	12.10	11.03	8.90	1.33	2.84
9	13.59	12.38	9.69	1.50	5.81
10	15.58	13.59	9.97	1.65	4.34

Table A3. NIAE for the instantaneous voltage or current value of Scheme A3 [compiled by the authors].

No.	THD_U, %	NIAE of Voltage, Harmonic Analysis, p.u. $\times 10^{-3}$	NIAE of Voltage, Spline Interpolation, p.u. $\times 10^{-3}$	NIAE of Current, Harmonic Analysis, p.u. $\times 10^{-3}$	NIAE of Current, Spline Interpolation, p.u. $\times 10^{-3}$
1	6.57	8.33	7.28	2.99	3.58
2	7.08	8.69	6.71	3.12	2.98
3	7.70	9.39	8.47	3.25	6.11
4	8.46	10.13	8.15	3.35	4.09
5	9.42	10.97	8.65	3.56	4.49
6	10.69	11.62	10.14	3.92	5.55
7	11.67	12.22	10.48	4.26	5.30
8	12.89	13.38	12.04	4.68	8.44
9	14.46	14.76	12.25	5.03	6.77
10	16.56	15.89	13.01	5.43	6.86

Table A4. NIAE for the instantaneous voltage or current value of Scheme B1 [compiled by the authors].

No.	THD_U, %	NIAE of Voltage, Harmonic Analysis, p.u. $\times 10^{-3}$	NIAE of Voltage, Spline Interpolation, p.u. $\times 10^{-3}$	NIAE of Current, Harmonic Analysis, p.u. $\times 10^{-3}$	NIAE of Current, Spline Interpolation, p.u. $\times 10^{-3}$
1	12.32	0.38	0.26	23.20	18.21
2	13.38	0.35	0.26	20.56	16.99
3	14.61	0.24	0.24	15.43	14.64
4	15.99	0.28	0.22	16.19	13.63
5	17.48	0.22	0.22	13.76	13.18
6	18.98	0.36	0.28	19.06	16.28
7	19.84	0.40	0.33	22.76	19.14
8	20.68	0.60	0.44	30.98	23.87
9	21.50	0.67	0.56	36.53	30.48
10	22.34	0.88	0.73	46.76	35.94

Table A5. NIAE for the instantaneous voltage or current value of Scheme B2 [compiled by the authors].

No.	THD_U, %	NIAE of Voltage, Harmonic Analysis, p.u. $\times 10^{-3}$	NIAE of Voltage, Spline Interpolation, p.u. $\times 10^{-3}$	NIAE of Current, Harmonic Analysis, p.u. $\times 10^{-3}$	NIAE of Current, Spline Interpolation, p.u. $\times 10^{-3}$
1	14.61	0.34	0.21	19.71	14.27
2	15.62	0.28	0.24	16.73	14.50
3	16.64	0.29	0.24	16.99	15.25
4	17.64	0.33	0.19	18.65	13.80
5	18.60	0.33	0.30	19.25	17.67
6	19.51	0.47	0.33	25.46	19.12
7	20.05	0.48	0.40	26.84	21.77
8	20.59	0.57	0.47	31.50	26.33
9	21.15	0.74	0.55	39.16	30.44
10	21.76	0.82	0.69	44.17	36.90

Table A6. NIAE for the instantaneous voltage or current value of Scheme B3 [compiled by the authors].

No.	THD_U, %	NIAE of Voltage, Harmonic Analysis, p.u. $\times 10^{-3}$	NIAE of Voltage, Spline Interpolation, p.u. $\times 10^{-3}$	NIAE of Current, Harmonic Analysis, p.u. $\times 10^{-3}$	NIAE of Current, Spline Interpolation, p.u. $\times 10^{-3}$
1	9.91	0.61	0.33	39.70	26.09
2	10.82	0.63	0.51	41.10	32.30
3	11.91	0.69	0.52	43.89	34.56
4	13.26	0.77	0.56	47.55	36.53
5	14.97	0.80	0.61	47.70	36.68
6	17.26	0.70	0.53	40.59	30.87
7	19.05	0.59	0.53	35.83	31.55
8	21.32	0.48	0.50	29.11	28.11
9	22.77	0.79	0.68	44.02	37.44
10	23.61	0.92	0.85	52.63	46.30

Table A7. NIAE for the instantaneous voltage or current value of Scheme B4 [compiled by the authors].

No.	THD_U, %	NIAE of Voltage, Harmonic Analysis, p.u.	NIAE of Voltage, Spline Interpolation, p.u.	NIAE of Current, Harmonic Analysis, p.u.	NIAE of Current, Spline Interpolation, p.u.
1	9.9	0.031	0.027	1.000	0.525
2	10.6	0.032	0.026	1.006	0.501
3	11.2	0.034	0.028	1.014	0.510
4	12.1	0.037	0.032	1.021	0.540
5	13.2	0.039	0.033	1.028	0.530
6	14.7	0.043	0.037	1.035	0.559
7	16.0	0.046	0.037	1.050	0.541
8	17.5	0.049	0.038	1.065	0.534
9	19.2	0.054	0.042	1.070	0.544
10	21.6	0.058	0.047	1.098	0.599

Table A8. NIAE for the instantaneous voltage or current value of Scheme B5 [compiled by the authors].

No.	THD_U, %	NIAE of Voltage, Harmonic Analysis, p.u.	NIAE of Voltage, Spline Interpolation, p.u.	NIAE of Current, Harmonic Analysis, p.u.	NIAE of Current, Spline Interpolation, p.u.
1	9.9	0.066	0.026	1.003	0.501
2	10.6	0.185	0.054	1.979	1.011
3	11.2	0.191	0.054	1.998	0.974
4	12.1	0.200	0.058	2.018	1.001
5	13.2	0.210	0.065	2.033	1.056
6	14.7	0.224	0.066	2.034	0.987
7	16.0	0.232	0.072	2.077	1.048
8	17.5	0.242	0.073	2.097	1.010
9	19.2	0.260	0.081	2.108	1.052
10	21.6	0.272	0.083	2.163	1.042

References

1. Rohouma, W.; Balog, R.S.; Peerzada, A.A.; Begovic, M.M. D-STATCOM for Harmonic Mitigation in Low Voltage Distribution Network with High Penetration of Nonlinear Loads. *Renew. Energy* **2020**, *145*, 1449–1464. [CrossRef]
2. Reguieg, Z.; Bouyakoub, I.; Mehedi, F. Harmonic Mitigation in Grid-Integrated Renewable Energy Systems with Nonlinear Loads. *Energy* **2025**, *324*, 135882. [CrossRef]
3. Ustinov, D.A.; Shafhatov, E.R. Assessment of Reliability Indicators of Combined Systems of Offshore Wind Turbines and Wave Energy Converters. *Energies* **2022**, *15*, 9630. [CrossRef]
4. Rodríguez-Pajarón, P.; Hernández, A.; Milanović, J.V. Probabilistic Assessment of the Impact of Electric Vehicles and Nonlinear Loads on Power Quality in Residential Networks. *Int. J. Electr. Power Energy Syst.* **2021**, *129*, 106807. [CrossRef]
5. Nishad, D.K.; Tiwari, A.N.; Khalid, S. A Comprehensive Analysis of Application Based Linear-Nonlinear Loads. In *Proceedings of the 2024 International Conference on Signal Processing and Advance Research in Computing (SPARC), Lucknow, India, 12 September 2024*; IEEE: New York, NY, USA, 2024; pp. 1–6. [CrossRef]
6. Skamyin, A.N.; Rastvorova, I.V. Consumed Power Regulation Algorithm in the Presence of High Harmonics. *J. Phys. Conf. Ser.* **2021**, *1753*, 012042. [CrossRef]
7. Taghvaie, A.; Warnakulasuriya, T.; Kumar, D.; Zare, F.; Sharma, R.; Vilathgamuwa, D.M. A Comprehensive Review of Harmonic Issues and Estimation Techniques in Power System Networks Based on Traditional and Artificial Intelligence/Machine Learning. *IEEE Access* **2023**, *11*, 31417–31442. [CrossRef]
8. Duc, M.L.; Bilik, P.; Martinek, R. Harmonics Signal Feature Extraction Techniques: A Review. *Mathematics* **2023**, *11*, 1877. [CrossRef]
9. Michalec, Ł.; Jasiński, M.; Sikorski, T.; Leonowicz, Z.; Jasiński, Ł.; Suresh, V. Impact of Harmonic Currents of Nonlinear Loads on Power Quality of a Low Voltage Network–Review and Case Study. *Energies* **2021**, *14*, 3665. [CrossRef]
10. Iliev, I.; Nazarychev, A.; Solovev, S.; Beloev, I.; Suslov, K.; Beloev, H. Reliability Assessment Methods for Power Supply Systems Considering the Technical Condition of Electrical Equipment: A Critical Review. *Energies* **2026**, *19*, 2440. [CrossRef]
11. Priyadarshini, M.S.; Bajaj, M.; Prokop, L.; Berhanu, M. Perception of Power Quality Disturbances Using Fourier, Short-Time Fourier, Continuous and Discrete Wavelet Transforms. *Sci. Rep.* **2024**, *14*, 3443. [CrossRef]
12. Zhukovskiy, Y.; Suslikov, P.; Rasputin, D. NILM-Based Feedback for Demand Response: A Reproducible Binary State-Detection Algorithm Using Active Power. *Electricity* **2026**, *7*, 23. [CrossRef]
13. Sychev, Y.A.; Zimin, R.Y.; Aladin, M.E. Analysis of Efficiency of Power Quality Maintenance by Multifunction Filter Compensating Devices Based on Several Active Converters in Combined Power Supply Systems in Mines. *Gorn. Zhurnal* **2025**, *9*, 44–51. [CrossRef]
14. Bogdanov, I.; Abramovich, B. Improving the Efficiency of Autonomous Electrical Complexes of Oil and Gas Enterprises. *J. Min. Inst.* **2021**, *249*, 408–416. [CrossRef]
15. Vasilev, B.U.; Nguyen, T.H. Influence of semiconductor converters on asynchronous drive battery and motor in mining machines. *Min. Inf. Anal. Bull.* **2023**, *9*, 299–318. [CrossRef]
16. *GOST 32144-2013*; Electric Energy. Electromagnetic Compatibility. The Quality Standards of Electric Energy in General-Purpose Power Supply Systems. Standartinform: Moscow, Russia, 2014.
17. *EN 50160:2022*; Voltage Characteristics of Electricity Supplied by Public Electricity Networks. CENELEC: Brussels, Belgium, 2022.

18. *IEEE 519-2014*; IEEE Recommended Practice and Requirements for Harmonic Control in Electric Power Systems. IEEE: Piscataway, NJ, USA, 2014.
19. Srivastava, A.K.; Tiwari, A.N.; Singh, S.N. Harmonic/Inter-Harmonic Estimation: Key Issues and Challenges. In *Proceedings of the 2021 IEEE 6th International Conference on Computing, Communication and Automation (ICCCA), Arad, Romania, 17 December 2021*; IEEE: New York, NY, USA, 2021; pp. 842–853. [CrossRef]
20. Elphick, S.; Gosbell, V.; Smith, V.; Perera, S.; Ciufo, P.; Drury, G. Methods for Harmonic Analysis and Reporting in Future Grid Applications. *IEEE Trans. Power Deliv.* **2017**, *32*, 989–995. [CrossRef]
21. Arranz-Gimon, A.; Zorita-Lamadrid, A.; Morinigo-Sotelo, D.; Duque-Perez, O. A Review of Total Harmonic Distortion Factors for the Measurement of Harmonic and Interharmonic Pollution in Modern Power Systems. *Energies* **2021**, *14*, 6467. [CrossRef]
22. Daniel, K.; Kütt, L.; Iqbal, M.N.; Shabbir, N.; Raja, H.A.; Sardar, M.U. A Review of Harmonic Detection, Suppression, Aggregation, and Estimation Techniques. *Appl. Sci.* **2024**, *14*, 10966. [CrossRef]
23. Aziz, M.H.A.; Azizan, M.M.; Sauli, Z.; Yahya, M.W. A Review on Harmonic Mitigation Method for Non-Linear Load in Electrical Power System. In *Proceedings of the Green Design and Manufacture 2020, Arau, Malaysia, 23–24 July 2020*; AIP Press: New York, NY, USA, 2021; p. 020022. [CrossRef]
24. Sychev, Y.; Zimin, R. Improving the Quality of Electricity in the Power Supply Systems of the Mineral Resource Complex with Hybrid Filter-Compensating Devices. *J. Min. Inst.* **2021**, *247*, 132–140. [CrossRef]
25. Vasilev, B.Y.; Nguyen, T.H. Stochastic Pulse-Width Modulation and Modification of Direct Torque Control Based on a Three-Level Neutral-Point Clamped Inverter. *Energies* **2024**, *17*, 6017. [CrossRef]
26. Mishra, M. Power Quality Disturbance Detection and Classification Using Signal Processing and Soft Computing Techniques: A Comprehensive Review. *Int. Trans. Electr. Energ. Syst.* **2019**, *29*, e12008. [CrossRef]
27. Karafotis, P.A.; Georgilakis, P.S. Power Quality Monitoring and Evaluation in Power Systems under Non-stationary Conditions Using Wavelet Packet Transform. *High Volt.* **2019**, *4*, 186–196. [CrossRef]
28. Islam, M.; Sanjeevikumar, P.; Brice, C.W. Redefined Power Quality Indices for Stationary and Nonstationary Power Quality Disturbances. In *Proceedings of the IECON 2019—45th Annual Conference of the IEEE Industrial Electronics Society, Lisbon, Portugal, 11–14 October 2019*; IEEE: New York, NY, USA, 2019; pp. 4019–4024. [CrossRef]
29. Skamyin, A.; Dobush, V.; Jopri, M. Determination of the Grid Impedance in Power Consumption Modes with Harmonics. *J. Min. Inst.* **2023**, *261*, 443–454. [CrossRef]
30. Nazarychev, A.N.; Minakova, T.E.; Popov, M.V. Results of Research into Interharmonics of Traction Electric Drive Systems for Mining Transport Machines. *Min. Ind. J.* **2025**, *1S*, 68–72. [CrossRef]
31. Coelho, R.D.A.; Brito, N.S.D. Power Measurement Using Stockwell Transform. *IEEE Trans. Power Deliv.* **2021**, *36*, 3091–3100. [CrossRef]
32. Su, T.; Yang, M.; Jin, T.; Flesch, R.C.C. Power Harmonic and Interharmonic Detection Method in Renewable Power Based on Nuttall Double-window All-phase FFT Algorithm. *IET Renew. Power Gen.* **2018**, *12*, 953–961. [CrossRef]
33. Liu, H.; Hu, H.; Chen, H.; Zhang, L.; Xing, Y. Fast and Flexible Selective Harmonic Extraction Methods Based on the Generalized Discrete Fourier Transform. *IEEE Trans. Power Electron.* **2018**, *33*, 3484–3496. [CrossRef]
34. Chen, J.; Wu, J.; Shi, B.; Chen, Q.; Fan, Y.; Fang, Y.; Wang, X. Parameter Identification for Magnetic-Geared Motors Combining Resonance Characteristics and BP-NN. *Measurement* **2026**, *290*, 122794. [CrossRef]
35. Aliukov, S.; Alabugin, A.; Osintsev, K. Review of Methods, Applications and Publications on the Approximation of Piecewise Linear and Generalized Functions. *Mathematics* **2022**, *10*, 3023. [CrossRef]
36. Asghari, M.; Fathollahi-Fard, A.M.; Mirzapour Al-e-hashem, S.M.J.; Dulebenets, M.A. Transformation and Linearization Techniques in Optimization: A State-of-the-Art Survey. *Mathematics* **2022**, *10*, 283. [CrossRef]
37. Pruski, P.; Paszek, S. Calculations of Power System Electromechanical Eigenvalues Based on Analysis of Instantaneous Power Waveforms at Different Disturbances. *Appl. Math. Comput.* **2018**, *319*, 104–114. [CrossRef]
38. Younis, R.; Reinhardt, A. A Study on Fundamental Waveform Shapes in Microscopic Electrical Load Signatures. *Energies* **2020**, *13*, 3039. [CrossRef]
39. Ezhov, N.; Neitzel, F.; Petrovic, S. Spline Approximation, Part 1: Basic Methodology. *J. Appl. Geod.* **2018**, *12*, 139–155. [CrossRef]
40. Howard, R.M. Dual Taylor Series, Spline Based Function and Integral Approximation and Applications. *Math. Comput. Appl.* **2019**, *24*, 35. [CrossRef]
41. Neitzel, F.; Ezhov, N.; Petrovic, S. Total Least Squares Spline Approximation. *Mathematics* **2019**, *7*, 462. [CrossRef]
42. Ali Abdulmohsin, H.; Bahjat Abdul Wahab, H.; Mohssen Jaber Abdul Hossen, A. A Novel Classification Method with Cubic Spline Interpolation. *Intell. Autom. Soft Comput.* **2022**, *31*, 339–355. [CrossRef]
43. Sun, F.; Cai, Z. Cubic Polishing Spline-Based Algorithms for Industrial Image Processing. *IEEE Trans. Ind. Inf.* **2024**, *20*, 314–326. [CrossRef]
44. Zhao, S.; Liu, Y. Waveform Quality Evaluation Method of Variable-Frequency Current Based on Curve Fitting. *Energies* **2022**, *15*, 7594. [CrossRef]

45. De La O Serna, J.A. Analyzing Power Oscillating Signals with the O-Splines of the Discrete Taylor–Fourier Transform. *IEEE Trans. Power Syst.* **2018**, *33*, 7087–7095. [CrossRef]
46. Aleixo, R.R.; Lomar, T.S.; Silva, L.R.M.; Monteiro, H.L.M.; Duque, C.A. Real-Time B-Spline Interpolation for Harmonic Phasor Estimation in Power Systems. *IEEE Trans. Instrum. Meas.* **2022**, *71*, 1–9. [CrossRef]
47. Deng, S.; Liu, Z.; Huang, L. A Signal Reconstruction Method Based on Quadratic Spline Interpolation Applied in Power Quality Analysis for SCM-TTU. *J. Phys. Conf. Ser.* **2020**, *1626*, 012055. [CrossRef]
48. Zeng, G.-Q.; Xie, X.-Q.; Chen, M.-R. An Adaptive Model Predictive Load Frequency Control Method for Multi-Area Interconnected Power Systems with Photovoltaic Generations. *Energies* **2017**, *10*, 1840. [CrossRef]
49. Kravchenko, V.F.; Churikov, D.V. Digital Signal Processing by Atomic Functions and Wavelets. *J. Commun. Technol. Electron.* **2023**, *68*, S1–S110. [CrossRef]

Disclaimer/Publisher's Note: The statements, opinions and data contained in all publications are solely those of the individual author(s) and contributor(s) and not of MDPI and/or the editor(s). MDPI and/or the editor(s) disclaim responsibility for any injury to people or property resulting from any ideas, methods, instructions or products referred to in the content.